# ELUCIDATING PHYSIOLOGY OF PLANT MEDIATED EXCHANGE PROCESSES USING AIRBORNE HYPERSPECTRAL REFLECTANCE MEASUREMENTS IN SYNOPSIS WITH EDDY COVARIANCE DATA

Michael Eiden[1], Sebastian van der Linden[2], Jan H. Schween[3], Christoph Gerbig[4], Bruno Neininger[5], Yves Brunet[6], Nathalie Jarosz[6], Olivier Traullé[7], Heiner Geiss[8] and Uwe Rascher[1*]

[1] Institute of Chemistry and Dynamics of the Geosphere, Institute III: Phytosphere, 52425 Jülich / Germany
[2] Geomatics Department, Humboldt-Universität zu Berlin, 10099 Berlin / Germany
[3] Institute of Geophysics and Meteorology, Cologne University, 50937, Cologne / Germany
[4] Max Planck Institute for Biogeochemistry, 07745 Jena / Germany
[5] Metair AG, 8915 Hausen am Albis / Switzerland
[6] INRA Domaine de la Grande-Ferrade BP 81 33883, Villenave-d'Ornon Cedex / France
[7] Meteo France, Centre National de Recherches Météorologiques, 31057 Cedex 1 Toulouse / France
[8] Institute of Chemistry and Dynamics of the Geosphere, Institute II: Troposphere, 52425 Jülich / Germany

**ABSTRACT:**

The Carbo Europe Regional Experiment Strategy (CERES), conducted between May and June 2005, aims to determine a spatially resolved regional balance of carbon dioxide fluxes using different methodological approaches bundled within an international framework. In this study we elucidated several meteorological and physiological parameters determining plant mediated exchange processes using airborne hyperspectral reflectance measurements in synopsis with meteorological information like eddy flux covariance data. We used an airborne hyperspectral system to record spatial and temporal transects of vegetated areas surrounding flux tower sites in the Bordeaux / Landes Region (France). Alongside hyperspectral measurements a comprehensive range of meteorological and surface flux parameters were measured at a flux tower site within the same time frame.
Unsupervised data analysis using cluster analysis was performed on predefined spectral wavelength windows. Additionally multiblock principal component analysis was used as explanatory data driven tool to reveal underlying data structures and to elucidate potential interdependencies between airborne hyperspectral reflectance data and meteorological ground measurements.
In detail temporal, physiological changes in relevant ground information like temperature, humidity, vegetation mediated $CO_2$ flux, latent heat flux or photosynthetic light use efficiency on the one hand and selected regions of the hyperspectral signatures, such as reflectance in the region of 531nm, which determines variations in the photochemical reflectance index (PRI) or in the spectral regions of chlorophyll fluorescence were examined.
Unsupervised cluster analysis revealed coupled dependencies between changes in the derivate spectra in the range of 720 to 740 nm with gross photosynthetic uptake rate, global radiation and time of day. Multiblock principal component analysis revealed that first derivative reflectance in wavelengths from 500 to 540 nm and between 680 and 750 nm had higher loading values in respect to observed ground variables global radiation and gross photosynthetic uptake rate respectively. The significance of these findings is discussed.

## 1. INTRODUCTION

Roughly 90% of the gas exchange between the atmosphere and the bio-geosphere is mediated by plants through stomata and photosynthesis regulation (Ozanne et al. 2003). Photosynthetic apparatus dynamically adapts to environmental constrains and efficiency of photosynthesis depends on the properties and local environment of individual leaves and is difficult to model on the ecosystem level. This causes substantial uncertainties in global carbon models (Running et al. 2000). Variations in light use efficiency (LUE) arise from diverse contributions of plant genetic, morphological and architectural components to core ecosystem functions such as carbon and water vapor fluxes, energy transfer, responses to changing environment, stress and nutrients. On the ground eddy covariance measurements (Baldocchi 2003) are an accepted approach to quantify

photosynthetic carbon uptake, but until now no reliable remote sensing approach exists to quantify the actual physiological status of photosynthesis.
Recent developments in sensor technology and remote sensing sciences may provide direct information to quantify photosynthetic efficiency directly. The photochemical reflectance index (PRI), which can be derived from hyperspectral reflectance measurements, was developed to serve as an estimate of photosynthetic efficiency (Gamon et al. 1993; 1997; Peñuelas et al. 1995). This normalized difference reflectance index uses two wavebands: 531 nm, which is affected by the conversion of two pigments that dynamically adapt to physiological changes in photosynthesis, and 570 nm, which serves as a reference (Gamon et al. 1992). PRI has been successfully used to detect changes in photosynthetic efficiency from the leaf to the ecosystem level (for an overview see

---
[*] Contact: u.rascher@fz-juelich.de

literature cited in Nichol et al. 2006; Rascher et al., 2007). However, effort is still needed to accurately scale these results to canopies, as absolute PRI values are greatly affected species properties (Guo & Trotter 2004) by structural properties, such as leaf angle distribution and seasonal changes in canopy structure (Barton & North 2000; Filella et al. 2004).

As a second promising approach to quantify physiology of photosynthesis is the detection of the fluorescence signal from chlorophyll a of the photosystems that is emitted with two specific maxima at 690 and 740 nm. Even though fluorescence is only 2-5 percent of the reflected light of green vegetation it still may be detectable using high performance hyperspectral sensors. The approach to use the sun-induced fluorescence signal as a measure of photosynthetic efficiency was recently highlighted by ESA's selection of the FLuorscence EXplorer (FLEX) mission to detect canopy fluorescence in the oxygen absorption bands from space (Carter et al., 1990, 1996; Cecchi et al., 1994; Moya et al. 2004)

In this communication we evaluated the potential to detect dynamic changes in canopy reflectance that is correlated to changes in photosynthesis. According to our knowledge this is the first publication combining airborne reflectance data from a natural canopies measured from different heights (100 - 2500 m), different times of the growing season, and different times of the day on the one hand, and ground measured data of photosynthesis on the other hand that was quantified by eddy covariance. In respect to the dynamic nature of photosynthesis, we also applied multiblock principal component analysis to our measurements. This method was originally developed in the field of chemometrics and is routinely used in the process monitoring approaches. Up to our knowledge this is the first time that multiblock principal component analysis is applied in the field of remote sensing with respect to plant physiology.

## 2. MATERIALS AND METHODS

### 2.1 Study site

The campaign was carried out in a 300 x 300 km large area in the South West of France belonging to the Départements Gironde and Landes. The region is dominated by commercially used pine forests, intensively used agricultural fields like maize and bean fields, as well as vineyards. The study site was chosen from a meteorological background, because of its steady westerly winds originating over the Atlantic Ocean. This allows an unbiased examination of changes in carbon dioxide concentration as air packages are moving eastwards over vegetated areas. Details about the experiment strategy and the study site are found in Dolman et al. 2006.

For this study we selected one field situated at 44°24' N and 0°38'22''W in a farmland site called La Cape Sud. The field approximately extents to 800 m in North-South direction and 500 m in East-West direction respectively in is traversed by to small ways used for farming activities. It is covered homogenously with Maize plants and watered artificially with use of an automatic irrigation system (Figure 1A).

### 2.2 Study period

Flights were conducted on 9 individual days within two distinct periods ranging from May 24th to May 27th and June 6th to June 17th, respectively. For some of the observation days, two separate flights were performed: one before noon and one in the afternoon. The data recorded on May 27th was chosen as sample data set, which was used to establish the data pre-processing

routine described in the following chapters. The generated routines were then applied to data of all other flights individually.

Altogether, the data pool generated in context of this study comprises out of more than 270.000 individual spectra and accompanying video images. In general, observations were made at flight altitudes between 100 and approx. 2500 m.



Figure 1:
(A) Intensive study site (maize field at La Cape Sud) with eddy covariance tower (back left) and irrigation system (right). The picture is taken at May 25th at the beginning of the measurements, thus showing lowest vegetation cover. (B) Hyperspectral reflectance sensor (FieldSpec Pro) mounted in an underwing pod of the Dimona research aircraft. The fibre optics is NADIR pointing with a synchronized video camera and data acquisition is imbedded in the aircrafts positioning and computer system.

### 2.3 Airborne hyperspectral measurements

The ECO-Dimona research aircraft from Metair AG (Menzingen, Switzerland) was used as platform for the hyperspectral measurements. Alongside an extensive range of meteorological parameters like $CO_2$, CO, NOx, (Neininger, 2001) were also captured simultaneously during flight. Additionally, for all measurements essential background information like flight altitude, position, and orientation was recorded. For the collection of hyperspectral reflectance data, a portable sensor (FieldSpec Pro, ASD Inc., Boulder, CO, USA) was mounted in the left under-wing pod of the aircraft (Figure 1B). Reflected light was captured in nadir orientation with a fiber optic that was equipped with a 1° lens barrel. Incident light was integrated for 130ms and spectrally analyzed in the range from 350 to 1050 nm, with a spectral resolution (FWHM) of 1.4 nm. The instrument was operated in continuous mode, thus spectra were collected with approximately 2 Hz. Spectral measurements were recorded using radiances and exposure time was adjusted to have best signal to noise ratio and to avoid saturation. In order to improve data quality, three spectra were averaged. A TTL trigger signal, generated by the FieldSpec device, was used (i) to record the time of each hyperspectral measurement and (ii) to capture a video image (640 x 480 pixels, 12-bit, grey values) using an industrial video camera (Flea, Point Grey Research, Vancouver, BC, Canada; with a 25

mm lens, Cosmicar/Pentax). Both camera and hyperspectral sensor share the same viewing orientation, but differ in their field of view (1° for the FieldSpec device and 10.5° for the video camera).

## 2.4 Eddy flux measurements

Meteorological ground measurements and calculation of turbulent fluxes was performed by Yves Brunet's Group from INRA (Institut national de la recherché agronomique / Bordeaux).

An eddy flux tower was installed and operated continuously in the centre of a maize field belonging to the faming site "La Cape Sud".

Flux measurements are related to friction velocity, energy budget and fluxes of trace species. The two former are measured together with the flux of $CO_2$. Considering the surface energy balance expressed as the distribution of net radiation $R_n$ into sensible heat flux (H), latent heat flux (LE), and ground heat flux (G), consists of a 3D sonic anemometer, an infrared gas analyzer measuring $CO_2$ and $H_2O$ concentrations, and several radiation sensors. Friction velocity (u*), H, LE and $CO_2$ flux were calculated using the eddy covariance technique, following a standardized protocol for instrument setup and data processing. The following instrumentation was used on the tower.

| Parameter | Instrument |
|---|---|
| $CO_2$ and $H_2O$ IRGA | Li-7500 (LICOR, Lincoln, NE, USA) |
| 3D-wind | Sonic Young 8100 |
| Horizontal wind speed | Cup anemometer (Cimel) |
| Wind direction | Campbell |
| Air temperature and humidity | Vaisala |
| Net radiation | NR-Lite |
| Global radiation | Cimel CE 180 |
| PPFD | Skye |
| Precipitation / irrigation | Several rain jauges |

Table 1: Flux tower instrumentation

## 3. DATA PRE-PROCESSING

### 3.1 Hyperspectral data pre-processing

To handle and access data effectively, fusion and organization strategies were developed. Since the location of all objects seen by the sensor is a function of the aircraft's position, altitude and orientation, an exact assignment of these parameters to the spectral measurements is implicitly necessary for accurate data correction and subsequent interpretation tasks. To tackle this challenge, we developed a scalable database like data structure, merging all measured information, synchronized via trigger signals and timestamps. In summary, each record consists of 750 data points, of which 701 are spectral reflectance values. The remaining 49 data points are comprised of background information like time, geometric information as well as of meteorological information measured at coincident time on the aircraft.

**Geometric correction:** To determine the ground "foot print" actually observed by the sensor, we reconstructed the relative viewing geometries for each measurement using the aircraft's altitude, GPS position, pitch, roll and azimuth angles as well as a digital elevation model. Furthermore unmeasured effects like updraft dependent wing flex of the aircraft were compensated, by comparing calculated "foot print" positions with corresponding video camera imagery, iteratively.

We are very confident to determine the foot print's center position with an accuracy of approximately 1/2 of its diameter. Also the exterior geometry, describing the photon path from the sun to the target and then to the observing sensor, was determined using the relative orientation in conjunction with astronomical information. Knowledge about the relative azimuth and sun elevation is important for the interpretation of bidirectional surface reflection characteristics. For further analyses we only used those reflectance measurements, which centre position was insured to be within the vegetation of the eddy flux site.

**Radiance to Reflection conversion:** To convert the measured radiance spectra into reflectance spectra, a normalizing approach was conducted. The most homogeneous spectral signature found within the study site was the "Dune de Pyla", Europe's largest wandering dune, located at the Atlantic coast at 44°35'40.0" North and 1° 12' 40.0" West in vicinity of the town Pyla sur Mer. The dune was recorded on many overpasses at varying altitudes during all flight days, due to the fact, that this area was chosen as a turning point in the flight patterns. Using sand as a reference is useful, because of its nearly "lambertian" reflection properties and its compositional homogeneity. Sand was collected from the dune and absolute reflection properties were determined under distinct laboratory conditions. Flight specific "radiance templates" were inferred using all available overpasses of the "Dune de Pyla". In order to compensate for varying ancillary conditions, like prevailing atmospheric conditions and sand humidity, radiance templates needed to be determined for each flight individually.

In a subsequent step, a conversion template was constructed using the quotient of the flight specific radiance template and the true reflection signature. Once this conversion template was computed, all other radiance spectra within the same time frame were converted to reflection spectra via division.

**Atmospheric correction**: Since the aircraft is moving in three dimensions and thus the photon pathway length is different for each measured spectrum, also atmospheric interactions are varying and needed to be compensated for individually. Atmospheric interactions underlie two fundamental principles: absorption and scattering.

Gaseous absorption occurs at well defined spectral bands depending on the molecular concentration of the absorbing gas within the radiation pathway (Schande, 1986). In our measured spectral signal, gaseous absorption is mainly caused from oxygen at 762 nm and water vapour at several broad spectral regions, mostly in the mid-infrared region. Since the focus of our work is dominated by plant interactions in the visible and near-infrared regions and information about the spatial and temporal variability of absorbing gases was not available, we decided to segment the spectral data to a range of 350 to 750 nm. Atmospheric scattering caused by molecules and aerosol particles, however has an additive effect (path radiance) on lower wavelength regions. This effect is dependent on the optical thickness of the atmosphere below the sensor and the prevailing aerosol conditions (Angstrom, 1964).

In order to describe and correct the additive scattering effects, we investigated the impact of scattering on the spectral signature of water, measured at different flight altitudes.

Roughly 2000 pure water measurements, originating from an area approximately 2 km west of the "Dune du Pyla" were extracted from the dataset. Similar to the dune measurements, these measurements were recorded at varying altitudes. For each wavelength we then investigated the height dependency and applied a robust regression fit to the minimal values. We chose the robust regression approach, because its liability for outliers is minimized compared to the traditional linear regression approach (Street et al, 1988). The height dependency of atmospheric scattering exhibits a nearly perfect linear relationship. Figure (2) depicts the robust regression fit for the wavelength of 350 nm.
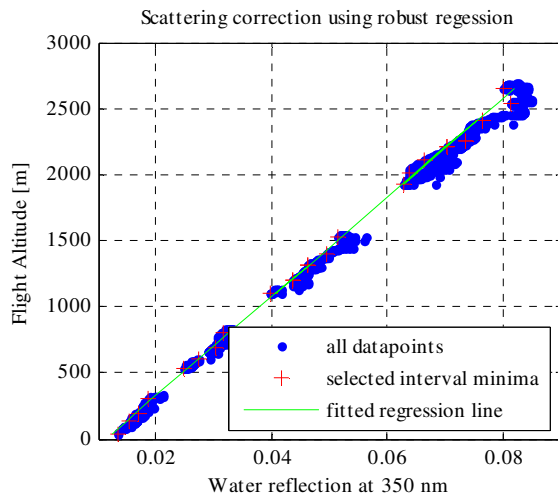


Figure 2:
Concept of height dependent atmospheric correction of reflectance data using robust regression.

For each wavelength, the robust regression approach determines a correction coefficient and a corresponding offset value. The correction coefficient describes the steepness of the fitted function and therefore characterizes the height dependent scattering effect. The offset value denotes the intersection point of the fitted function with the wavelength axis.
It shows that the height dependent influence of scattering decreases in an almost linear way as observed wavelengths increase Figure (3A). Furthermore it shows, that this effect is expanding far into the visual range and thus, might influence single-band based vegetation indices like the photochemical reflectance index (PRI), the cartenoid reflectance index (CRI) and the anthocyanin reflectance index (ARI) and others, if not corrected properly.
In our case the minimal regression coefficient is found at 572 nm, showing that, at this wavelength, the slightest height dependent effect can be determined. Coefficients for wavelengths greater than the minimal value show no apparent structure, due to the fact no longer scattering but other processes like gaseous absorption are predominating. Therefore, we decided to restrict the scattering correction to the range of 350 to 572 nm, shown in blue in Figure (Figure 3B).
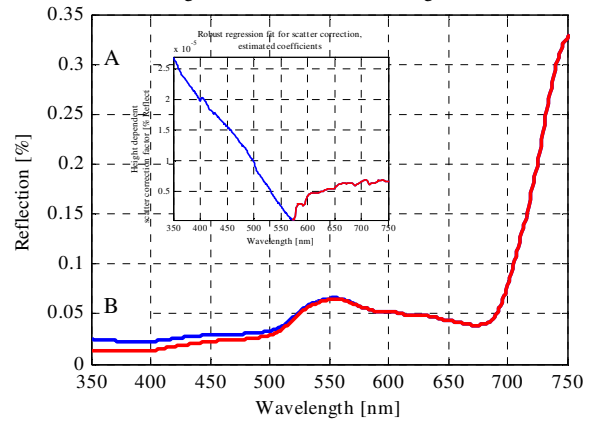


Figure 3.
Derived correction coefficients (3A) and comparison of uncorrected (blue) and corrected vegetation spectra (3B)

Similar to the conversion from radiance to reflection values, the atmospheric scatter correction was computed for each flight individually. The correction itself was performed by subtracting the product of the determined coefficient with a given height from the original reflection values for wavelengths from 350 to 572 nm.

**Absolute and derivative spectra:** For further analyses we calculated two data sets: one consisting of absolute reflectance data (Figure 4A) and a second one containing the first derivatives of the reflectance data (Figure 4B). Derivative spectra may display narrow waveband features more obvious and are less dependent from changes in intensity of incoming radiation. In order to suppress high frequency noise, we smoothed the derivative spectra using a 15nm Savitzy-Golay smoothing function (Savitzky & Golay, 1965).
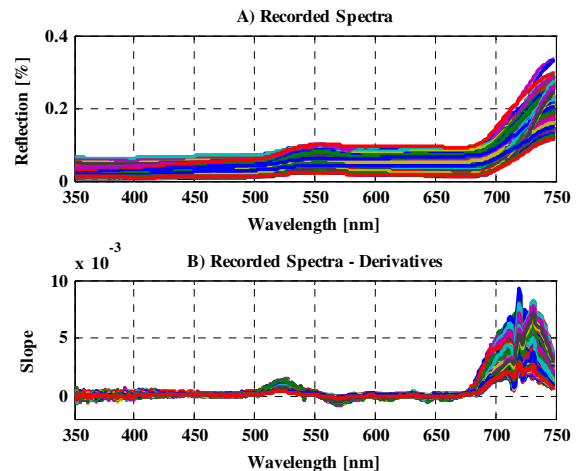


Figure 4.
Reflectance data that were selected and used for statistical analyses. Altogether roughly 500 spectra were selected after pre-processing (A) original spectra and (B) 1st derivative spectra after smoothing with 15nm Savitzy-Golay filter.

### 3.2 Pre-processing of meteorological ground measurements

Similar to the spectral measurements also the meteorological ground measurements required intense data pre-processing procedures described in the following paragraphs.

**Elimination of un reliable fluxes:** The quality of the measured turbulent fluxes is highly dependent on the meteorological conditions. During times with very low wind velocities, turbulence coefficients may be affected by measurement artifacts like flow distortion by the instrument itself, or the influence of small surface inhomogeneities in the direct vicinity of the instrument. Therefore we decided not to use data taken at wind velocities below 2 m/s. Furthermore all data were pre-processed using a 2 hour smoothing filter.

**Eddy flux footprint:** The flux footprint i.e. the surface area where the flux mainly originates from changes its size and location with prevailing wind conditions and thermal stratification of the air. Therefore this footprint is not necessarily identical with the location and direct vicinity of the eddy covariance station itself. In order to ensure, that the inferred fluxes are mediated by fields observed by the airborne sensor we estimated the temporal variability of the flux foot print location and size using the wind direction and velocity. In a subsequent step we only selected those flux measurements, where wind direction ensured a footprint lying within the observed vegetation.
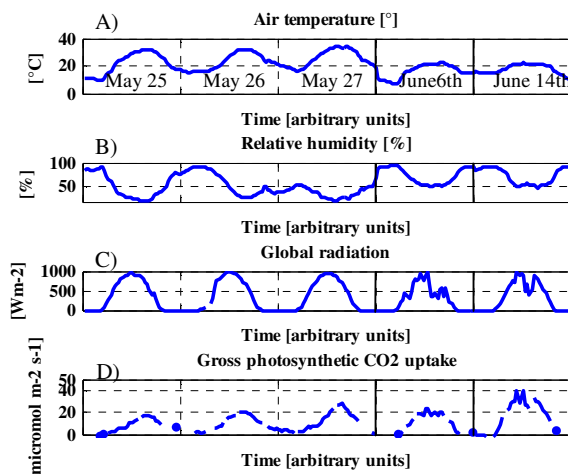


Figure 5.

Environmental factors and photosynthetic $CO_2$ uptake rate of the studied corn field at the days of overflights. Air-temperature (A), relative humidity (B), and global incoming radiation (C) were measured on the eddy flux tower. Net photosynthetic $CO_2$ uptake rate (D) were calculated from temperature corrected $CO_2$ flux data (see text for procedure)

**Inferring gross photosynthetic uptake rate from data:** Since the carbon dioxide exchange rate is comprised of photosynthesis as well as soil respiration the latter part needed to be subtracted in order to achieve gross photosynthetic uptake rate. Therefore an empirical correction scheme was conducted using the nightly carbon dioxide fluxes and soil temperature. As long as water status remains constant, microbial activity in soil and root respiration is mainly temperature dependent. We used all night time $CO_2$ flux data obtained during the measurement period and plotted those as a function of soil temperature.

Exponential rise of $CO_2$ fluxes with temperature and a linear correlation in Arrhenius plot supported this approach, the derived Q10 value was 1.14. From this night time data a temperature corrected estimate of soil respiration was derived and temperature corrected respiration was subtracted from net carbon fluxes yielding photosynthetic $CO_2$ uptake rates and meteorological and environmental parameters determining plant performance.

## 4. DATA ANALYSIS

Hyperspectral measurements were linked to meteorological information measured on the ground via unique timestamps. After all pre-processing and merging procedures, the dataset consisted out of almost 500 data instances comprising out of two the distinct data blocks.

We treat both airborne hyperspectral and ground based measurements as independent approaches, both characterizing vegetation and its response to changing environmental conditions. Analysis of the data blocks and their interdependencies was conducted using two different approaches.

### 4.1 Forward search for interdependencies between spectral and ground data

We investigated the spectral variability in numerous predefined spectral wavelength windows using an unsupervised data analysis approach.

In detail eight spectral windows (350 – 500 nm, 500 – 600 nm, 600 – 670 nm, 680 – 750 nm, 526 -536 nm, 565 – 575 nm, 680 - 700nm and 720 - 740nm) were analyzed separately.

Absolute and first derivative spectra were partitioned into 5 clusters using Ward's algorithm (Ward, 1963) (5 different colors lower panel of Figure (6) In parallel the histogram distribution of ground measured variables were computed (see upper right panel in Figure (6) for the histogram distribution of photosynthetic $CO_2$ uptake rate). The interrelation of the two data sets was inspected visually on color coded cluster histograms (upper left panel in Figure (6) shows the cluster partitions and their and their corresponding composition of photosynthetic uptake rate status).

In this example it shows, that cluster 4 and 5, which are related to each other according to the dendrogram plot (data not shown) contain more samples measured at higher photosynthetic uptake rates (i.e. > 27 $\mu$mol m$^{-2}$ s$^{-1}$) as clusters 1 to 3, where lower values are dominating. Furthermore Cluster 5 shows no contamination from samples acquired at lower photosynthetic uptake rates.
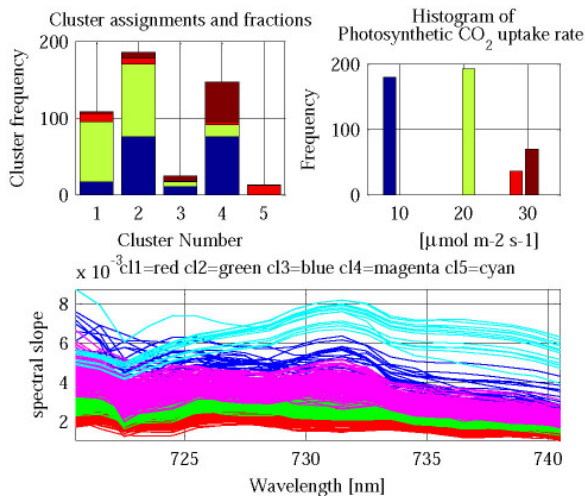
Figure 6

Example output from unsupervised analysis with spectral data colorcoded in cluster assignments (lower panel), cluster distribution and their corresponding combination of selected ground data variable fractions (upper right), histogram distribution of selected ground data variable (upper left).

### 4.2 Reverse search for interdependencies between spectral and ground data

In this context we performed multiblock-PCA approach to elucidate potential dependencies between the two distinct blocks. The multiblock-PCA approach is an extension of the traditional principal component analysis and was originally developed in field of chemometrics (Westerhuis et al, 1998). It aims at revealing underlying phenomena between predefined data blocks both describing the same object. For example, the blocks can be defined as datasets of two different analytical techniques both investigating the same sample.

Firstly the algorithm performs a traditional principal component analysis on each data block separately in order to decompose the dataset into a set of few uncorrelated and independent factors. In a subsequent step the resulting scores and factors for both PCA approaches are then subjected to additional PCA on a so called super level.

The multiblock analysis can be used as an explanatory tool and has the advantage it requires no a priori information. One drawback of the multiblock approach is that all data need to be normalized and scaled before projection in order to avoid artefacts due to pre-processing.

In the context of this study spectral data was used in a window from 350 up to 750 nm. For the ground data, a set of variables most strongly linked to plant activity was pre-selected. Among them were: gross photosynthetic uptake rate, global radiation, air temperature, relative humidity and latent heat flux.

## 5. RESULTS

### 5.1 Forward approach:

According to the visual inspection described in the previous chapter, no obvious dependencies between absolute reflectance data and ground data could be observed. (Table 2)

Slight dependencies could also be detected for flight altitude, manifesting in lower wavelength region, which was assumed to be most like due to remaining atmospheric scattering effects. Additionally a possible dependency between derivative

reflectance in the 720 – 740 nm window with photosynthetic uptake rate (Figure 6). , global radiation and time of day could be observed The three parameters: photosynthetic uptake rate, global radiation and time of day are intercorrelated, i.e. global radiation is highest during midday, which also facilitates highest rates of photosynthetic $CO_2$ uptake. Thus, it's motivating that these three parameters also appear correlated in this analysis.

| Original Spectra / First derivate Spectra | 350-500nm | 500-600nm | 600-670nm | 680-750nm | 526-536nm | 565-575nm | 680-700nm | 720-740nm |
|---|---|---|---|---|---|---|---|---|
| Flight altitude [m] | + | - | - | - | - | - | - | - |
|  | - | - | - | - | - | - | - | - |
| Zenith difference [°] | - | - | - | - | - | - | - | - |
|  | - | - | - | - | - | - | - | - |
| Azimuth difference [°] | - | - | - | - | - | - | - | - |
|  | - | - | - | - | - | - | - | - |
| Time of day | - | - | - | - | - | - | - | - |
|  | - | - | - | - | - | - | - | ++ |
| Absolute time | - | - | - | - | - | - | - | - |
|  | - | - | - | - | - | - | - | - |
| Air temperature [°C] | - | - | - | - | - | - | - | - |
|  | - | - | - | - | - | - | - | - |
| Wind velocity [m/s] | - | - | - | - | - | - | - | - |
|  | - | - | - | - | - | - | - | - |
| Global radiation | - | - | - | - | - | - | - | - |
|  | - | - | - | - | - | - | - | ++ |
| Relative humidity [%] | - | - | - | - | - | - | - | - |
|  | - | - | - | - | - | - | - | - |
| Photosynthetic uptake rate [$\mu mol\ m^{-2}\ s^{-1}$] | - | - | - | - | - | - | - | - |
|  | - | - | - | - | - | - | - | ++ |

Table 2:
Dependencies as identified by the forward cluster analyses. '+' / '++' indicate a weak / apparent dependency between two parameters and '-' indicates no dependency. Dependencies were described by visual inspection of the results.

### 5.2 Reverse approach:

Since the multiblock analysis is a purely data driven projection method, it provides a more objective view of inherent dependencies of the two independently measured data sets. In this context we used it to reveal common structures inherent in both data sets.

For the "ground data" block it showed, that for Factor 1 the variable "global radiation" indicates the highest loading value (i.e. contribution) compared to gross photosynthetic uptake rate, air temperature, relative humidity, and latent heat flux. In

Factor 2 the variable "photosynthetic uptake rate" is predominating (data not shown).

Since we are primarily interested, which spectral features might be coherent with the observed findings in the ground data block, we examined the super level scores and weights (data not shown) and the corresponding spectral loading plots of those factors found to be most closely linked to the factors determined in the ground data block.
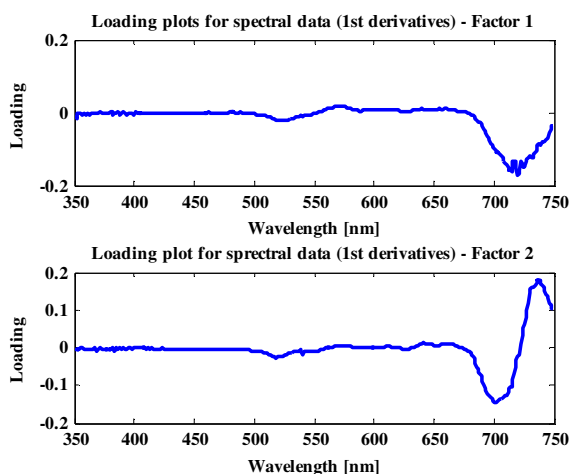


**Figure 7:**
Spectral loading plots, depicting the contribution of wavelengths to the Factors determined by principal component analysis.

The first Factor computed on derivative spectra was found to be most strongly linked to Factor 1 in the "ground data block" (i.e dominated by global radiation), whereas the second one was found to be most strongly linked to Factor 2 in the ground data block (i.e dominated by photosynthetic uptake rate).

The underlying structure of the spectral loading plots revealed, that wavelengths contribute differently to the observed patterns. In spectral data block a contribution of the derivative spectra between 500 and 540 nm and above 680 nm at first factor was clearly observed. Surprisingly at factor 2 a complex 2-peak feature above 670 nm appeared .

## 6. DISCUSSION

With this communication we demonstrate that variations in canopy reflectance that occur in the range of 500-550 nm and 680-750 nm may be associated with changes in canopy photosynthetic carbon fixation measured on the ground. These inter-correlations were detected with two independent statistical methods and only occurred in these wavebands. Whereas the forward analysis approach is highly subjective, the multiblock principal component approach requires no a priori knowledge. The changes could not simply be explained by the increased leaf area index of the vegetation within the whole measuring period. Thus our results point towards dynamic changes in reflectance in these spectral regions during the course of the day and changes that are driven by changing illumination (see Table 2).

During the past years a lot of effort was put in the search for a suitable method to directly measure photosynthetic efficiency to reduce uncertainties in carbon models (Running et al 2000) and

for managing agricultural systems. Up to now two approaches are favored and our results may well contribute in better planning future experiments and to focus on the potentially best spectral regions.

As a first approach hyperspectral reflectance measurements show increasing potential for monitoring function of plant ecosystems. The photosynthetic reflectance index (PRI) positively correlates with photosynthetic efficiency, is negatively correlated with NPQ and has been successfully used to detect changes in photosynthesis on the leaf level (Peñuelas *et al.*, 1995; 1997; Gamon *et al.*, 1997) and small canopy level (Gamon *et al.*, 1992; Stylinski *et al.*, 2002; Trotter *et al.*, 2002, Nichol et al. 2006). However, on the ecosystem high uncertainties arise and only a very few studies are available that could reliably correlate variations of PRI with ecosystem photosynthesis (Nichol *et al.*, 2000; 2002). Other studies explicitly report that they failed to predict photosynthetic efficiency using the PRI (Methy, 2000) or structural changes in the canopy superimposed subtle changes in photosynthetic efficiency.

A second remote sensing approach attempts to directly measure the fluorescence signal of chlorophyll that is closely related to charge separation within the photosystems itself and that can be used to quantify carbon metabolism (Rascher et al 2004). Fluorescence of chlorophyll is emitted as a two peak feature that is related to the physiological status of photosynthesis (see introduction for references). Despite this obvious advantage it still remains a challenge to detect the comparably small variations in fluorescence on the background of reflected and scattered light. Additionally the link between canopy fluorescence and ecosystem carbon exchange still needs to be made.

We acknowledge the uncertainties that still underlie our analyses and we want to point out that the limited data pool and a possible bias in data distribution has to be reevaluated. Thus, our study should be understood as a first promising evaluation of both approaches. Greatly extended measurements will take place in 2007 in the same study site. During these studies additional airborne sensors will be employed, auxiliary ground data will be acquired and care will be taken to avoid bias in the data sets.

But we clearly could demonstrate the potential of the multiblock approach that revealed subtle and unsupervised dependencies between ground measured photosynthesis and airborne and ultimately spaceborne reflectance.

We propose that the fluorescence signal is the superior signature because variations in reflectance at 680-750 nm had a greater contribution to explain variations on the ground (Fig. 7) and the fact that a two-peak feature emerged in this region might point towards the underlying fluorescence that modulate reflectance in this region.

**REFERENCES**

Angstrom, A. (1964), Techniques of determining the turbidity of the atmosphere, *Tellus*, 13, 214, 1

Baldocchi D.D. (2003) Assessing the eddy covariance technique for evaluating carbon dioxide exchange rates of ecosystems: past, present and future. *Global Change Biology*, 9: 479-492.

Barton, C.V.M., and P.R.J. North (2000). Remote sensing of canopy light use efficiency using the photochemical reflectance index. *Remote Sensing of Environment*, 78: 264-273.

Carter, G.A., Jones, J.H. Mitchell R.J., and Brewer C.H. (1996). Detection of solar-excited chlorophyll a fluorescence and leaf photosynthetic capacity using a Fraunhofer line radiometer. *Remote Sensing of Environment*, 55: 89-92.

Carter G.A. Theisen A.F. Mitchell R.J. (1990) Chlorophyll fluorescence measured using the Fraunhofer line-depth principle and relationship to photosynthetic capacity in the field. *Plant, Cell & Environment* 13, 79-83

Cecchi, G., Manzzinghi, P., Pantani, L., Valentini, R., Tirelli, D., & De Angelis., P. (1994). Remote sensing of chlorophyll a fluorescence of vegetation canopies: 1. Near and far field measurement techniques. *Remote Sensing of Environment*, 47, 18-28

Dolman A. J. et al. (2006), "CERES, the CarboEurope Regional Experiment Strategy in Les Landes, South West France, May-June 2005". *BAMS Atmospheric Chemistry*, in press.

Filella I. Peñuelas J. Llorens L. Estiarte M. (2004) Reflectance assessment of seasonal and annual changes in biomass and $CO_2$ uptake of a Mediterranean shrubland submitted to experimental warming and drought. *Remote Sensing of Environment* 90, 308-318.

Gamon, J.A., I. Filella, and J. Peñuelas, (1993). The dynamic 531-nm Δ reflectance signal: a survey of 20 angiosperm species. Photosynthetic responses to the environment (H.Y. Yamamoto and C.M. Smith, editors), *American Society of Plant Physiologists*, Rockville, MD, pp. 172-177.

Gamon, J.A., J. Peñuelas, and C.B. Field, (1992). A narrow-waveband spectral index that tracks diurnal changes in photosynthetic efficiency. *Remote Sensing of Environment*, 41: 35-44.

Gamon, J.A., L. Serrano, and J.S. Surfus, (1997). The photochemical reflectance index: an optical indicator of photosynthetic radiation use efficiency across species, functional types and nutrient levels. *Oecologia*, 112: 492-501.

Guo J. and Trotter C.M. (2004) Estimating photosynthetic light-use efficiency using the photochemical reflectance index: variations among species. *Functional Plant Biology* 31, 255 - 265.

Methy, M., 2000. Analysis of photosynthetic activity at the leaf and canopy levels from reflectance measurements: a case study. *Photosynthetica*, 38: 505-512.

Moya I. Camenen L. Evain S. Goulas Y. Cerovic Z.G. Latouche G. Flexas J. Ounis A. (2004) A new instrument for passive remote sensing: 1. Measurements of sunlight-induced chlorophyll fluorescence. *Remote Sensing of Environment* 91, 186-197.

Neininger, B. (2001), "A small aircraft for more than just ozone: Metair's 'Dimona' after ten years of evolving development". *Proceedings of the 11th Symposium on Meteorological Observations and Instrumentation*, 81st AMS Annual Meeting, 14-19 January 2001, Albuquerque, NM, USA.

Nichol, C.J., K.F. Hümmrich, T.A. Black, P.G. Jarvis, C.L. Walthall, J. Grace, and F.G. Hall, 2000. Remote sensing of photosynthetic-light-use efficiency of boreal forest. *Agricultural and Forest Meteorology*, 101: 131-142.

Nichol, C. J., J. Lloyd, O. Shibistova, A. Arneth, C. Roser, A. Knohl, S. Matsubara, and J. Grace, 2002. Remote sensing of photosynthetic light use efficiency of Siberian boreal forest *Tellus B*, 54: 677-687.

Nichol C.J., Rascher U., Matsubara S. & Osmond C.B. (2006) Assessing photosynthetic efficiency in an experimental mangrove canopy using remote sensing and chlorophyll fluorescence Trees – *Structure and Function*, 20, 9-15.

Ozanne CMP, Anhuf D, Boulter SL, Keller M, Kitching RL, Meinzer FC, Mitchell AW, Nakashizuka T, Dias PLS, Wright SJ & Yoshimura M (2003) Biodiversity meets the atmosphere: a global view of forest canopies. *Science* 301, 183-186.

Peñuelas, J., I. Filella, and J.A. Gamon, 1995. Assessment of photosynthetic radiation-use efficiency with spectral reflectance. *New Phytologist*, 131: 291-296.

Peñuelas, J., J. Llusia, J. Pinol, and I. Filella, 1997. Photochemical reflectance index and leaf radiation-use efficiency assessment in Mediterranean trees. *International Journal of Remote Sensing*, 13: 2863-2868.

Rascher U., Bobich E.G., Lin G.H., Walter A., Morris T., Naumann M., Nichol C.J., Pierce D., Bil K., Kudeyarov V. & Berry J.A. (2004) Functional diversity of photosynthesis during drought in a model tropical rainforest – the contributions of leaf area, photosynthetic electron transport and stomatal conductance to reduction in net ecosystem carbon exchange. *Plant, Cell & Environment*, 27, 1239-1256.

Rascher U., Nichol C.L., Small C. & Hendricks L. (2007) Monitoring spatio-temporal dynamics of photosynthesis with a portable hyperspectral imaging system. A case-study to quantify photosynthetic efficiency on genetically modified Arabidopsis thaliana (L.) Heynh. plants and on leaves of four drought stressed tropical tree species. *Photogrammetric Engineering and Remote Sensing*, 73, 45-56.

Running SW, Thornton PE, Nemani R & Glassey JM, (2000) Global terrestrial gross and net primary productivity from the earth observing system. In: Sala OE, Jackson RB, Mooney HA & Howarth RW (eds) *Methods in Ecosystem Science* Springer Verlag, New York, pp 44-57.

Savitzky, A., and Golay Marcel J.E. ,(1964). Smoothing and Differentiation of Data by Simplified Least Squares Procedures. *Analytical Chemistry*, 36: 1627-1639

Schande, E., (1988), *Physical Fundamentals of Remote Sensing,* Springer-Verlag, New York, 1986

Stylinski, C.D., J.A. Gamon, and W.C. Oechel, (2002). Seasonal patterns of reflectance indices, carotenoid pigments and photosynthesis of evergreen chaparral species. *Oecologia*, 131: 366-374.

Street, J.O. et al, (1988), A Note on Computing Robust Regression Estimates via Iteratively Reweighted Least Squares. *The American Statistician*, 42, p.152-154.

Trotter, G.M., D. Whitehead, and E.J. Pinkney, (2002). The photochemical reflectance index as a measure of photosynthetic light use efficiency for plants with varying foliar nitrogen content. *International Journal of Remote Sensing*, 23: 1207-1212.

Ward, J., (1963), Hierarchical Grouping to optimize an objective function, *Journal of American Statistical Association*, 58(301)

Westerhuis, J., Kourti, T., Macgregor, J.F., (1998), Analysis of multiblock and hierarchical PCA and PLS models, *Journal of Chemometrics* 12, 301-321